Synthesis and Photoluminescence Properties of 2D Phenethylammonium Lead Bromide Perovskite Nanocrystals

Rui Guo, Zhuan Zhu, Abdelaziz Boulesbaa, Fang Hao, Alexander Puretzky, Kai Xiao, Jiming Bao, Yan Yao, and Wenzhi Li**

Organic–inorganic hybrid perovskites have emerged as promising optoelectronic materials for applications in photovoltaic and optoelectronic devices. Particularly, 2D layer-structured hybrid perovskites are of great interest due to their remarkable optical and electrical properties, which can be easily tuned by selecting suitable organic and inorganic moieties during the material synthesis. Here, the solution-phase growth of a large square-shaped single-crystalline 2D hybrid perovskite, phenethylammonium lead bromide $(C_6H_5C_2H_4NH_3)_2PbBr_4$ (PEPB), with thickness as few as 3 unit cell layers is demonstrated. Compared to bulk crystals, the 2D PEPB nanocrystals show a major blueshifted photoluminescence (PL) peak at 409 nm indicating an increase in bandgap of 40 meV. Besides the major peak, two new PL peaks located at 480 and 525 nm are observed from the hybrid perovskite nanocrystals. PEPB nanocrystals with different thicknesses show different colors, which can be used to estimate the thickness of the nanocrystals. Time-resolved reflectance spectroscopy is used to investigate the exciton dynamics, which exhibits a biexponential decay with an amplitude-weighted lifetime of 16.7 ps. The high-quality 2D $(C_6H_5C_2H_4NH_3)_2PbBr_4$ nanocrystals are expected to have high PL quantum efficiency and potential applications for light-emitting devices.

1. Introduction

The organic–inorganic lead halide perovskites, especially $CH_3NH_3PbI_3$, have gained substantial attention owing to their application in the solution-processed photovoltaic devices that have reached over 22% power conversion efficiency.[1,2] Compared to the 3D structured $CH_3NH_3PbI_3$, an organic cation with size bigger than three C—C or C—N bonds would potentially form a layered structure with distinct optical properties.[3] These layered organic–inorganic lead halide perovskite crystals have a general form of A_2PbX_4, where A is an organic ammonium or diammonium and X is a halide. Unit cells composed of one inorganic layer sandwiched between two organic layers are stacked up via van der Waals interactions between adjacent organic tails and form a long-range-ordered structure. Due to the difference between the dielectric constants of the organic and inorganic moieties, the dielectric confinement effect leads to an increased exciton binding energy and hence strong photoluminescence (PL).[4–6] The bulk materials of layered perovskites have been well studied since 1990s and largely increased exciton binding energy has been observed in $(C_6H_5C_2H_4NH_3)_2PbI_4$,[4] $(C_6H_5C_2H_4NH_3)_2PbBr_xI_{4-x}$,[6] $(C_6H_5C_2H_4NH_3)_2PbCl_xI_{4-x}$,[7] and $(C_6H_5C_2H_4NH_3)_2PbBr_xCl_{4-x}$.[8]

The layered perovskite forms a semiconductor/insulator multi-quantum-well system within which the inorganic semiconducting sheets composed of PbX_6^{4-} octahedra act as the wells and the surrounding insulating organic layers act as barriers.[9] Such systems provide electronic and optical properties different from bulk materials.[10–24] Benefiting from the flexibility of material selection of both the organic and inorganic moieties, a variety of atomically thin films of organic–inorganic perovskite materials can be synthesized to form a library of 2D materials.[7,25] Vertical and lateral heterostructures can be prepared, opening up intriguing possibilities for the design of materials with distinctive new properties at atomic scale.[10,13,15,17,18,26] Both light-emitting diodes and planar solar cells based on solution-processed perovskite multiple quantum wells have been demonstrated with high external quantum efficiency (QE) and high stability in ambient environment with encapsulation, respectively.[27,28] Compared to the bulk material, the study on nanostructured perovskite materials has just started.[10,12,13,15,16,26,29] Colloidal nanocrystals of 2D perovskite

R. Guo, Prof. W. Li
Department of Physics
Florida International University
Miami, FL 33199, USA
E-mail: wenzhi.li@fiu.edu

R. Guo, Dr. Z. Zhu, F. Hao, Prof. J. Bao, Prof. Y. Yao
Department of Electrical and Computer Engineering
University of Houston
Houston, TX 77204, USA
E-mail: yyao4@uh.edu

Dr. A. Boulesbaa, Dr. A. Puretzky, Prof. K. Xiao
Center for Nanophase Materials Sciences
Oak Ridge National Laboratory
Oak Ridge, TN 37831, USA

Prof. Y. Yao
Texas Center for Superconductivity at the University of Houston
Houston, TX 77204, USA

The ORCID identification number(s) for the author(s) of this article can be found under https://doi.org/10.1002/smtd.201700245.

DOI: 10.1002/smtd.201700245

materials have been synthesized by using long cation to arrest crystal growth in certain dimensions[12,13,15,30,31] or by antisolvent-solvent extraction process.[14] Nanosheets or nanoflakes of 2D perovskites can also be produced by mechanical exfoliation.[32,33] Recently, Dou et al. obtained atomically thin 2D $(C_4H_9NH_3)_2PbBr_4$ perovskite material by solution-phase growth method and a significantly increased PL QE of ≈26% (compared to <1% for bulk material) was observed which was attributed to the increase of the oscillator strength and the decrease of the nonradiative Auger recombination process in atomically thin 2D structures.[34]

Here, we demonstrate the synthesis of a new 2D organic–inorganic perovskite nanocrystals of phenethylammonium lead bromide (PEPB), $(C_6H_5C_2H_4NH_3)_2PbBr_4$, using solution-phase growth method. Uniform square-shaped 2D PEPB nanocrystals were synthesized successfully on SiO_2/Si substrates. Pyramid structure formed on top of PEPB sheets was observed and the thickness of PEPB monolayer was calculated to be 1.8 nm by averaging the step heights of the pyramid. Over 50% of the synthesized 2D PEPB nanocrystals were composed of less than 30 layers. The photoluminescence showed a major band-edge emission at 409 nm which slightly blueshifted compared to that of the bulk single crystal. Besides the major photoluminescence peak, the PEPB nanocrystals exhibited two new PL peaks at ≈480 and 525 nm which were not observed in bulk single crystals. The new PL peaks could probably be attributed to the radiative decay of organic part. Time-resolved reflectance contrast was measured and the result showed a broad induced absorption peak around 600 nm, attributed to the excited state, with an amplitude-weighted lifetime of 16.7 ps.

2. Results and Discussion

A schematic illustration in **Figure 1**A shows the chemical structure of a monolayer of PEPB. Each Pb atom is positioned inside an octahedral cage formed by six Br atoms and every in-plane Br atom is shared by the adjoining $PbBr_6^{4-}$ octahedra. The $(C_6H_5C_2H_4NH_3)_2PbBr_4$ unit cell self-assembles into a 2D sheet of corner-shared $PbBr_4^{2-}$ which lies in between two layers of organic moieties consisted of $C_6H_5C_2H_4NH_3^+$. The 2D nanocrystals of PEPB grown on SiO_2/Si substrates were examined by optical microscopy and the result is shown in Figure 1B. Blue square-shaped 2D nanocrystals with edge length around 5 µm could be easily distinguished from the purple background of substrate. Some square-shaped 2D PEPB nanocrystals can have edge length up to 30 µm. Atomic force microscopy (AFM) measurement showed that the thickness of these nanocrystals varied from a few nanometers to around 100 nm, with the corresponding color in the optical microscopy images changing from blue to yellow. AFM image of one PEPB nanocrystal showed a thickness of ≈9.1 nm (Figure 1C). The thinnest 2D crystal was measured to be ≈5.7 nm (±0.2 nm) thick.

It should also be noted that a pyramid-shaped structure was occasionally formed on top of some of the PEPB nanocrystals with thickness over 20 nm. Figure 1D shows such a pyramid formed on a 20 nm thick crystal. Figure 1E shows the

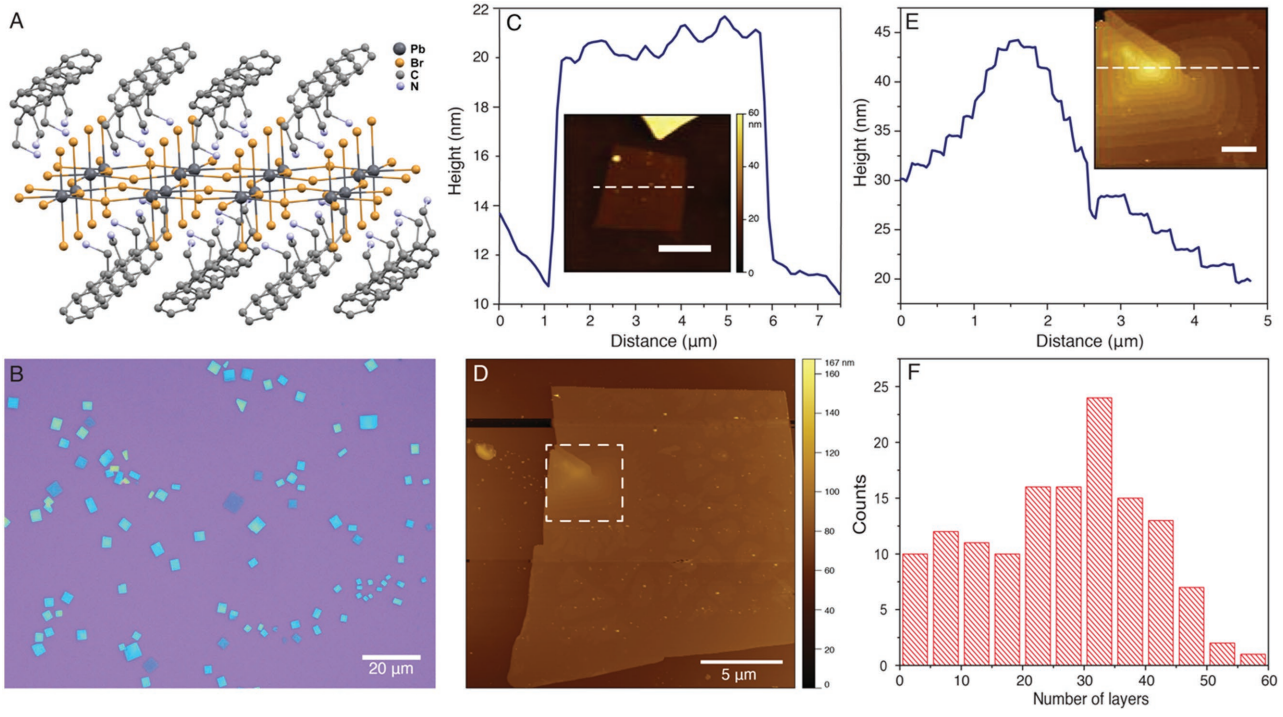

Figure 1. 2D $(C_6H_5C_2H_4NH_3)_2PbBr_4$ crystals. A) Structural illustration of a single layer $(C_6H_5C_2H_4NH_3)_2PbBr_4$ (PEPB) (black balls: lead atoms; gold balls: bromine atoms; gray balls: carbon atoms; light blue balls: nitrogen atoms; H atoms were removed for clarity). B) Bright field optical image of the 2D PEPB nanocrystals on SiO_2/Si substrate. C) Height profile of a 2D PEPB nanocrystal. The inset shows the AFM image with scale bar of 3 µm. D) AFM image of a pyramid formed on top of a PEPB nanocrystal. E) Height profile of the pyramid. A magnified image of the pyramid is shown in the inset. Scale bar in the inset: 2 µm. F) Thickness distribution statistics of 2D PEPB nanocrystals synthesized on SiO_2/Si substrates.

height profile of the pyramid as shown in the inset, which is a close-up view of the boxed area in Figure 1D. The inset in Figure 1E showed a clear layer-by-layer structure with each layer in a rounded rectangle shape. AFM measurement in Figure 1E showed that the height of each step was less than 2 nm. Considering that the *d*-spacing of PEPB bulk single crystal is 1.67 nm,[25] each step of the pyramid in the AFM image should be corresponding to one monolayer of PEPB. From the AFM measurement, the average height of each step, i.e., the thickness of PEPB monolayer, was ≈1.8 nm (±0.3 nm). This number is larger than the *d*-spacing of the bulk PEPB crystals. The larger thickness measured from AFM could be resulted from the settings of the tapping mode of the AFM, which was intended to avoid the sample damage. The relaxation of the organic moiety located at the top of PEPB nanocrystals could also contribute to the increased height. The height profile indicated that the very top step of the pyramid was only ≈0.8 nm thick (Figure 1E). It could probably be a sublayer of $C_6H_5C_2H_4NH_3Br$ bonded to the PEPB layer beneath it by van der Waals force. After measuring the thicknesses of 137 crystals synthesized using the same solution-phase growth procedure on 7 SiO_2/Si substrates by AFM, the distribution of the number of layers of 2D PEPB nanocrystals was calculated and presented in a histogram in Figure 1F. The thickest nanocrystal had a total of 60 layers, the thinnest one had only 3 layers, and over half of the nanocrystals had less than 30 layers (≈54 nm). The possibility to obtain 2D PEPB nanocrystals with 30–35 layers was nearly 20%, which was the highest, while the possibility to obtain nanocrystals with more than 50 layers was merely 2%, which was the lowest.

The PL properties of individual PEPB nanocrystal on SiO_2/Si substrates were investigated by using a UV-LED filtered by 365 nm bandpass as an excitation light source. **Figure 2**A displays the PL spectra of the bulk single crystal of PEPB and 2D nanocrystals with different thicknesses grown on SiO_2/Si substrate. The bulk single crystal shows a PL peak at 414 nm (2.99 eV) and the nanocrystals have blueshifted peaks at ≈409 nm (3.03 eV). The bandgap of 2D PEPB nanocrystals increased for 40 meV compared to the bulk single crystal. The increase of the bandgap is probably due to the relaxation and expansion of the $PbBr_4^{2-}$ frame within which the Pb—Br—Pb bond between adjoining $PbBr_6^{4-}$ octahedra was distorted in bulk single crystal.[25,34] The PL spectra peaks of both bulk single crystal and nanocrystals are asymmetric indicating the existence of multiple excitonic states or the coupling of excitons to phonons.[35]

To further study the photoluminescence of the 2D PEPB nanocrystals, a 405 nm wavelength laser diode was used as a strong photoexcitation source and a 410 nm long-pass filter was used to block the laser signal as well as the strong PL peak at ≈410 nm. Two new PL peaks located at around 480 and 525 nm and a shoulder located at around 448 nm were observed for the nanocrystals as shown in Figure 2B. With the increase of the thickness of the nanocrystals, these two PL peaks became shallow and wide. The 480 nm peak almost disappeared in the PL spectrum of the thickest nanocrystal. The same PL tests were also performed on the PEPB bulk single crystal samples and these PL peaks were not observed in the spectra. Recently, Blancon et al. reported PL emission with less energy than the bandgap from the layer-edge-states of the exfoliated $(C_4H_9NH_3)_2(CH_3NH_3)_{n-1}Pb_nI_{3n+1}$ nanocrystals with n = 3–5. However, for the n = 1 nanocrystal, i.e., $(C_4H_9NH_3)_2PbI_4$, PL emission from the layer-edge-states was not observed.[36] Therefore, for our 2D PEPB nanocrystals in which the n = 1, the two PL peaks at 480 and 525 nm were probably not the result of the radiative recombination of the layer-edge-states. It is speculated that these new PL peaks in our 2D PEPB nanocrystals probably originate from the radiative decay of the excited organic part which might indicated the energy/charge transfer between the inorganic and organic moieties after excitation. Theoretical calculation may help to confirm our hypothesis.

To study the dynamic processes of the absorption, time-resolved reflectance contrast change (RCC) of the 2D PEPB nanocrystals prepared on SiO_2/Si substrates were measured following the photoexcitation at 405 nm. We note that RCC

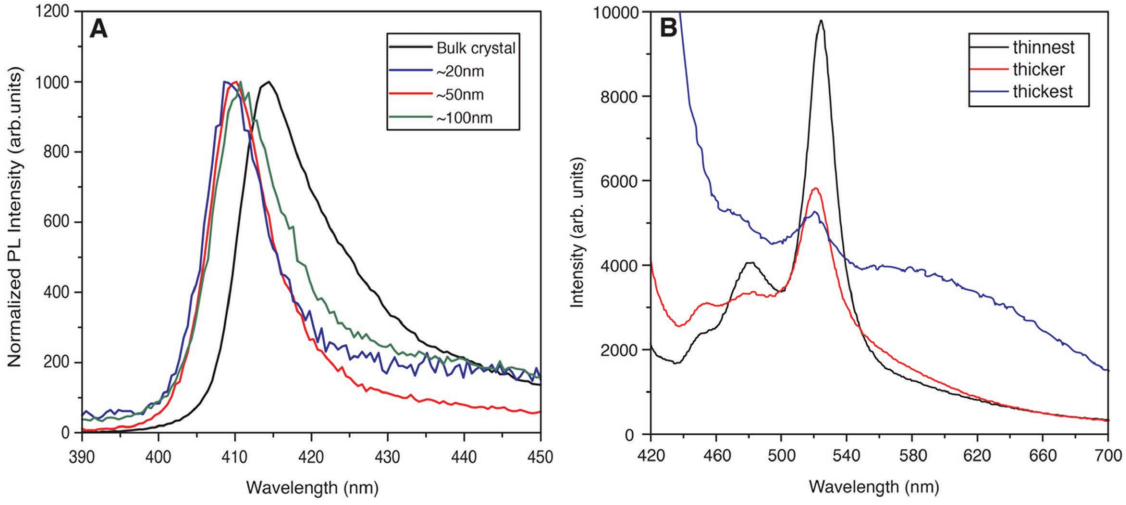

Figure 2. PL properties of the 2D $(C_6H_5C_2H_4NH_3)_2PbBr_4$ nanocrystals. A) Steady-state PL spectra of a piece of bulk crystal and three 2D $(C_6H_5C_2H_4NH_3)_2PbBr_4$ nanocrystals measured using a UV-LED source. B) PL peaks of three 2D nanocrystals located at 480 and 525 nm, obtained using a 405 nm laser as excitation and a 410 nm long-pass filter.

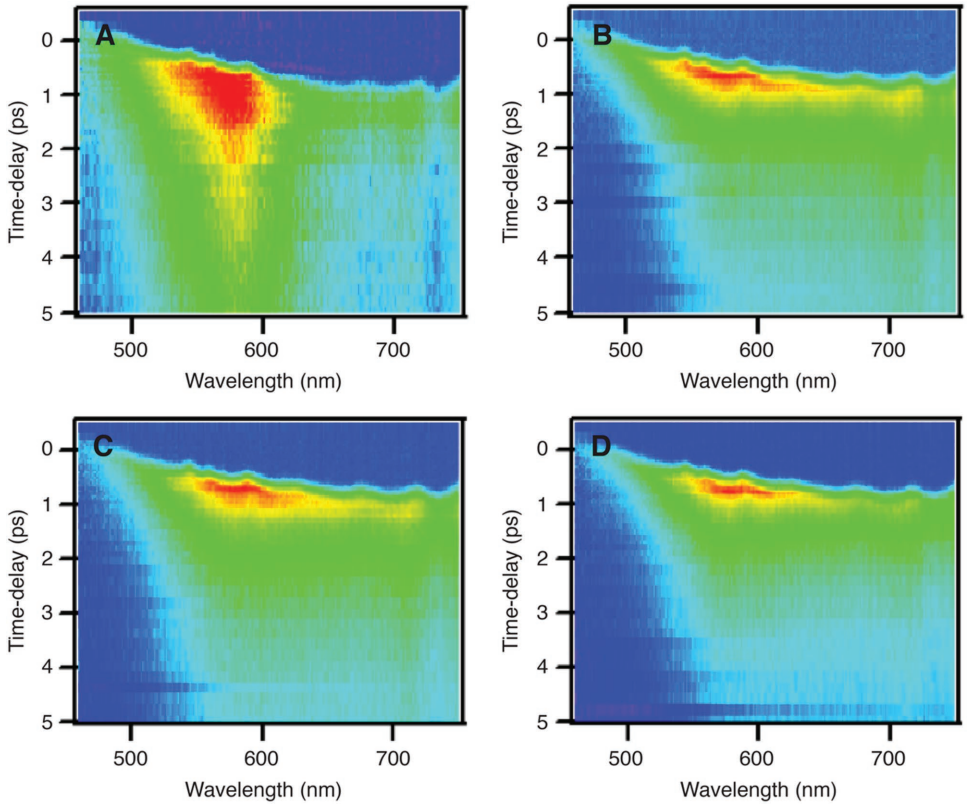

Figure 3. A–D) Time-resolved reflectance contrast of four 2D $(C_6H_5C_2H_4NH_3)_2PbBr_4$ nanocrystals.

signal at each time delay is calculated as RCC = $-[(R - R_0)/R_0] \times 100$, where R and R_0 are the intensities of the reflected probe with the pump on and off, respectively. **Figure 3** shows the results of four different 2D PEPB nanocrystals with different thicknesses. The results showed a broad positive RCC peak between 500 and 650 nm (red colored area in Figure 3) indicating an induced absorption attributed to the excited state. It is clear that the RCC signal shown in Figure 3A had a longer lifetime than that in Figure 3B–D although we are not able to correlate the thickness of these samples to their RCC signals in this report. **Figure 4**A is the RCC measurement up to 100 ps time-delay. The amplitude of the induced excited state absorption following the 405 nm excitation increased up to 3 times. To calculate the lifetime of the excited state, the decay of excited state-induced absorption signal averaged around 600 nm was fitted to a biexponential decay function convoluted with a Gaussian excitation pulse with 45 fs pulse duration (Figure 4B). The converged fitting result showed two time constants of 2.0 and 33.3 ps with an amplitude-weighted lifetime of $\tau \approx 16.7$ ps (**Table 1**).

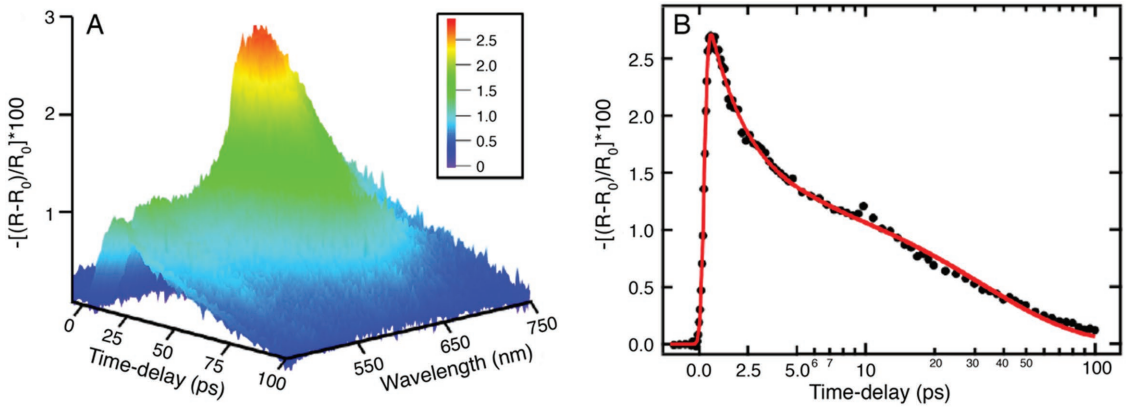

Figure 4. A) Time-resolved reflection contrast change up to 100 ps time-delay. B) Dynamics of the induced absorption signal averaged around the peak at 600 nm (symbols). The experimental data are fitted to a biexponential decay function (solid line).

Table 1. Parameters returned by the converged fit to the decay of the excited state induced absorption signal shown in Figure 4B. A_i (%) and T_i (ps) are the amplitude and the time constant of the exponential decay component *i*. The amplitude-weighted lifetime τ is calculated as $\tau = \frac{\sum_i A_i T_i}{\sum_i A_i}$.

A_1 [%]	T_1 [ps]	A_2 [%]	T_2 [ps]	τ [ps]
53	2.0	47	33.3	16.7

3. Conclusions

Here, we have presented solution-processed organic–inorganic hybrid 2D PEPB perovskite nanocrystals and a fundamental study on the exciton dynamics of the new 2D perovskite material utilizing photoluminescence and time-resolved reflectance measurements. Square-shaped 2D PEPB nanocrystals have been synthesized with edge length up to 30 µm and thickness of a few of tens of nanometers. The pyramid structure formed by PEPB on top of thin sheet was observed. The average height of the steps in the pyramid structure suggested that the thickness of a single layer of the PEPB nanocrystal was ≈1.8 nm (±0.3 nm), which was significantly larger than the *d*-spacing (1.67 nm) of PEPB bulk single crystal. The distribution of the number of layers of synthesized PEPB nanocrystals showed that over half of them were composed of less than 30 layers and that it is practical to obtain thin nanocrystals with few layers. The PL results have shown that the 2D nanocrystals of PEPB exhibited an asymmetric PL peak at 409 nm, slightly blueshifted compare to the PL peak of PEPB single crystal. Besides, two new PL peaks at 480 and 525 nm were observed from the 2D PEPB nanocrystals and they were probably resulted from the radiative decay in the organic moiety of the material indicating energy/charge transfer between inorganic and organic moieties. Time-resolved reflectance measurements showed a broad induced absorption peak, attributed to the excited state. The lifetime of the excited state was calculated to be 16.7 ps by fitting the decay of the induced absorption signal to a biexponential decay function.

4. Experimental Section

Phenethylamine ($C_6H_5C_2H_4NH_2$) and lead bromide ($PbBr_2$) were purchased from Sigma-Aldrich. Hydrobromic acid (HBr, 48%, w/w aq. solution) was purchased from Alfa Aesar. All chemicals were used as received.

Synthesis of $C_6H_5C_2H_4NH_3Br$: First, 5 mL of phenethylamine and 30 mL of ethanol were mixed and stirred in a 250 mL 2-neck flask in an ice-water bath. Then, 6.79 mL of HBr acid (48 wt% in water) was slowly added into the mixture. The mixture was stirred for 2 h at 0 °C maintained using an ice-water bath. The resulting solution was evaporated by a rotary evaporator at 70 °C to remove the solvent (ethanol and water), and white precipitate was formed. The white precipitate was then washed with diethyl ether by stirring for 30 min and collected by vacuum filtration, a step which was repeated three times. After filtration, the obtained $C_6H_5C_2H_4NH_3Br$ white powder was collected and dried in a vacuum oven at 60 °C overnight.

Growth of 2D $(C_6H_5C_2H_4NH_3)_2PbBr_4$ (PEPB) Nanocrystals: All the solution preparation and nanocrystals growth process were carried out in a nitrogen-filled glove box. The as-synthesized $C_6H_5C_2H_4NH_3Br$ (404.2 mg, 2 mmol) and $PbBr_2$ (367 mg, 1 mmol) were dissolved in 4 mL of anhydrous dimethylformamide (DMF). The solution was then diluted 100 times by a DMF/chlorobenzene (1:1 volume ratio) cosolvent resulting in a solution with a Pb^{2+} concentration of 2.5 mmol L^{-1}. Prior to use, 50 µL as-diluted solution was mixed with 527.8 µL chlorobenzene and 547.2 µL acetonitrile. SiO_2/Si substrates were cleaned by ultrasonication in isopropyl alcohol, acetone, deionized water, and isopropyl alcohol for 5 min, respectively; then dried by a nitrogen gun. Before use, the substrates were treated by UV-Ozone for 15 min, then transferred into a glovebox and preheated at 75 °C for 5 min on a hot plate. Finally, 3 µL of the above diluted precursor solution was dropped onto the surface of the substrate and dried at 75 °C for 5 min. Thin square-shaped nanocrystals of PEPB grew spontaneously on the surface of the substrate as the solvent evaporated.

Growth of $(C_6H_5C_2H_4NH_3)_2PbBr_4$ (PEPB) Single Crystals: To start the synthesis, 36.7 mg of $PbBr_2$ and 40.42 mg of as-synthesized $C_6H_5C_2H_4NH_3Br$ were added into 0.2 mL of HBr acid (48 wt% in water). The mixture was heated up and maintained at 120 °C until all the solids were dissolved. The solution was then slowly cooled down overnight and small white plate-like $(C_6H_5C_2H_4NH_3)_2PbBr_4$ crystals were precipitated. The crystals were then collected, washed with ethanol, and dried in vacuum oven overnight at 60 °C overnight.

Atomic Force Microscopy: Tapping mode AFM (Veeco Instrument, Inc.) measurements were performed to characterize the sizes and thicknesses of the 2D PEPB nanocrystals on SiO_2/Si substrates. Imaging was performed with antimony (*n*) doped silicon tips (TESPA, Brukerprobes) of 125 µm in length with a typical spring constant of 42 N m^{-1} and drive frequency of 320 kHz. During imaging, the height images of both forward and reverse scan directions, amplitude image, and phase image were collected simultaneously at a constant scan rate of 0.5 Hz. Gwyddion 2.47 was used to analyze the height images and to obtain particle sizes.

Photoluminescence Measurement: The photoluminescence spectra of the 2D PEPB nanocrystals were measured using HORIBA iHR320 Spectrometer equipped with thermoelectric cooling Synapse CCD. A 365 nm UV LED with a bandpass filter was used as excitation source. The light beam was focused onto the sample by a 100× objective lens and the photoluminescence signal was collected by the same objective lens. Long pass filters were applied to block the 365 nm component. The measurement was done at ambient temperature ≈25 °C and relative humidity in the range of 40–45%.

Time-Resolved Reflectance Measurements: The measurements were carried out on a home-built femtosecond pump–probe spectrometer (PPS). A full description of the PPS can be found elsewhere.[37] Briefly, the PPS is based on a titanium sapphire (Ti:Sa) oscillator (Micra, Coherent) with its output seeded by a Ti:Sa coherent legend (USP-HE) amplifier operating at 1 kHz repetition rate. This amplifier produces pulses centered at 800 nm with ≈45 fs duration and 2.2 mJ energy per pulse. The pump pulse at 400 nm is the second harmonic of the fundamental output of the legend amplifier. A small portion (≈2 µJ) of the beam from the Legend amplifier was focused onto a 2 mm thick sapphire window to generate the white light continuum probe, which covers a spectral region from 450 to 950 nm. On the sample, the pump and probe spot sizes were ≈7 mm. The pump fluence was kept below 2 µJ cm^{-2}. A spectrograph (Shamrock 303i, Andor) coupled with a CCD (Andor Newton) equipped with an electron multiplier was used for detecting the reflected white light probe. At each time delay between the pump and the probe, the percentage change in the reflectance contrast $\Delta R/R$ (%) was calculated as $100 \times (R - R_0)/R_0$, where R and R_0 are the intensities of the reflected probe with pump on and off, respectively.

Acknowledgements

W.L. acknowledges the funding from the National Science Foundation (Grant Nos. CMMI-1334417 and DMR-1506640). Y.Y. acknowledges the TcSUH core funding and the National Science Foundation (No. CMMI-1400261). J.B. acknowledges support from the Robert A. Welch Foundation (E-1728). The time-resolved reflectance and part of the

photoluminescence measurements were conducted at the Center for Nanophase Materials Sciences, which is a DOE Office of Science User Facility.

Conflict of Interest

The authors declare no conflict of interest.

Keywords

2D nanocrystals, organic–inorganic hybrid perovskites, photoluminescence, time-resolved reflectance spectroscopy

Received: July 12, 2017
Published online: September 13, 2017

[1] W. S. Yang, J. H. Noh, N. J. Jeon, Y. C. Kim, S. Ryu, J. Seo, S. I. Seok, *Science* **2015**, *348*, 1234.
[2] D.-Y. Son, J.-W. Lee, Y. J. Choi, I.-H. Jang, S. Lee, P. J. Yoo, H. Shin, N. Ahn, M. Choi, D. Kim, N.-G. Park, *Nat. Energy* **2016**, *1*, 16081.
[3] S. A. Veldhuis, P. P. Boix, N. Yantara, M. Li, T. C. Sum, N. Mathews, S. G. Mhaisalkar, *Adv. Mater.* **2016**, *28*, 6804.
[4] X. Hong, T. Ishihara, A. V. Nurmikko, *Phys. Rev. B* **1992**, *45*, 6961.
[5] M. Shimizu, J.-I. Fujisawa, J. Ishi-Hayase, *Phys. Rev. B* **2005**, *71*, 205306.
[6] K. Nobuaki, *Jpn. J. Appl. Phys.* **1997**, *36*, 2272.
[7] K. Nobuaki, *Jpn. J. Appl. Phys.* **1996**, *35*, 6202.
[8] N. Kitazawa, *J. Mater. Sci. Eng. B* **1997**, *49*, 233.
[9] J. Even, L. Pedesseau, C. Katan, *ChemPhysChem* **2014**, *15*, 3733.
[10] D. Sapori, M. Kepenekian, L. Pedesseau, C. Katan, J. Even, *Nanoscale* **2016**, *8*, 6369.
[11] S. Ahmad, G. V. Prakash, *J. Nanophotonics* **2014**, *8*, 083892.
[12] Q. A. Akkerman, S. G. Motti, A. R. Srimath Kandada, E. Mosconi, V. D'Innocenzo, G. Bertoni, S. Marras, B. A. Kamino, L. Miranda, F. De Angelis, A. Petrozza, M. Prato, L. Manna, *J. Am. Chem. Soc.* **2016**, *138*, 1010.
[13] Y. Bekenstein, B. A. Koscher, S. W. Eaton, P. Yang, A. P. Alivisatos, *J. Am. Chem. Soc.* **2015**, *137*, 16008.
[14] R. Naphade, S. Nagane, G. S. Shanker, R. Fernandes, D. Kothari, Y. Zhou, N. P. Padture, S. Ogale, *ACS Appl. Mater. Interfaces* **2016**, *8*, 854.
[15] J. A. Sichert, Y. Tong, N. Mutz, M. Vollmer, S. Fischer, K. Z. Milowska, R. Garcia Cortadella, B. Nickel, C. Cardenas-Daw, J. K. Stolarczyk, A. S. Urban, J. Feldmann, *Nano Lett.* **2015**, *15*, 6521.
[16] O. Vybornyi, S. Yakunin, M. V. Kovalenko, *Nanoscale* **2016**, *8*, 6278.
[17] A. B. Wong, M. Lai, S. W. Eaton, Y. Yu, E. Lin, L. Dou, A. Fu, P. Yang, *Nano Lett.* **2015**, *15*, 5519.
[18] Y. Xu, Q. Chen, C. Zhang, R. Wang, H. Wu, X. Zhang, G. Xing, W. W. Yu, X. Wang, Y. Zhang, M. Xiao, *J. Am. Chem. Soc.* **2016**, *138*, 3761.
[19] D. Zhang, S. W. Eaton, Y. Yu, L. Dou, P. Yang, *J. Am. Chem. Soc.* **2015**, *137*, 9230.
[20] S. Zhang, G. Lanty, J.-S. Lauret, E. Deleporte, P. Audebert, L. Galmiche, *Acta Mater.* **2009**, *57*, 3301.
[21] Y. Zhang, J. Liu, Z. Wang, Y. Xue, Q. Ou, L. Polavarapu, J. Zheng, X. Qi, Q. Bao, *Chem. Commun.* **2016**, *52*, 13637.
[22] K. Zheng, K. Žídek, M. Abdellah, M. E. Messing, M. J. Al-Marri, T. Pullerits, *J. Phys. Chem. C* **2016**, *120*, 3077.
[23] H. Zhu, Y. Fu, F. Meng, X. Wu, Z. Gong, Q. Ding, M. V. Gustafsson, M. T. Trinh, S. Jin, X. Y. Zhu, *Nat. Mater.* **2015**, *14*, 636.
[24] S. Zhuo, J. Zhang, Y. Shi, Y. Huang, B. Zhang, *Angew. Chem., Int. Ed.* **2015**, *54*, 5693.
[25] N. Kawano, M. Koshimizu, Y. Sun, N. Yahaba, Y. Fujimoto, T. Yanagida, K. Asai, *J. Phys. Chem. C* **2014**, *118*, 9101.
[26] S.-T. Ha, C. Shen, J. Zhang, Q. Xiong, *Nat. Photonics* **2015**, *10*, 115.
[27] N. Wang, L. Cheng, R. Ge, S. Zhang, Y. Miao, W. Zou, C. Yi, Y. Sun, Y. Cao, R. Yang, Y. Wei, Q. Guo, Y. Ke, M. Yu, Y. Jin, Y. Liu, Q. Ding, D. Di, L. Yang, G. Xing, H. Tian, C. Jin, F. Gao, R. H. Friend, J. Wang, W. Huang, *Nat. Photonics* **2016**, *10*, 699.
[28] Y. Chen, Y. Sun, J. Peng, W. Zhang, X. Su, K. Zheng, T. Pullerits, Z. Liang, *Adv. Energy Mater.* **2017**, https://doi.org/10.1002/aenm.201700162.
[29] S. Gonzalez-Carrero, G. M. Espallargas, R. E. Galian, J. Pérez-Prieto, *J. Mater. Chem. A* **2015**, *3*, 14039.
[30] L. Protesescu, S. Yakunin, M. I. Bodnarchuk, F. Krieg, R. Caputo, C. H. Hendon, R. X. Yang, A. Walsh, M. V. Kovalenko, *Nano Lett.* **2015**, *15*, 3692.
[31] L. C. Schmidt, A. Pertegás, S. González-Carrero, O. Malinkiewicz, S. Agouram, G. Mínguez Espallargas, H. J. Bolink, R. E. Galian, J. Pérez-Prieto, *J. Am. Chem. Soc.* **2014**, *136*, 850.
[32] O. Yaffe, A. Chernikov, Z. M. Norman, Y. Zhong, A. Velauthapillai, A. van der Zande, J. S. Owen, T. F. Heinz, *Phys. Rev. B* **2015**, *92*, 045414.
[33] X. Wu, M. T. Trinh, X. Y. Zhu, *J. Phys. Chem. C* **2015**, *119*, 14714.
[34] L. Dou, A. B. Wong, Y. Yu, M. Lai, N. Kornienko, S. W. Eaton, A. Fu, C. G. Bischak, J. Ma, T. Ding, N. S. Ginsberg, L.-W. Wang, A. P. Alivisatos, P. Yang, *Science* **2015**, *349*, 1518.
[35] K. Gauthron, J. S. Lauret, L. Doyennette, G. Lanty, A. Al Choueiry, S. J. Zhang, A. Brehier, L. Largeau, O. Mauguin, J. Bloch, E. Deleporte, *Opt. Express* **2010**, *18*, 5912.
[36] J.-C. Blancon, H. Tsai, W. Nie, C. C. Stoumpos, L. Pedesseau, C. Katan, M. Kepenekian, C. M. M. Soe, K. Appavoo, M. Y. Sfeir, S. Tretiak, P. M. Ajayan, M. G. Kanatzidis, J. Even, J. J. Crochet, A. D. Mohite, *Science* **2017**, *355*, 1288.
[37] A. Boulesbaa, K. Wang, M. Mahjouri-Samani, M. Tian, A. A. Puretzky, I. Ivanov, C. M. Rouleau, K. Xiao, B. G. Sumpter, D. B. Geohegan, *J. Am. Chem. Soc.* **2016**, *138*, 14713.

